Journal of
Computational and Theoretical Nanoscience
Vol. 9, 1–6, 2012

Evolution of Quantum Cellular Automata in Graphene Nanoribbons

A. León[1,*], M. Pacheco[1,2], and Z. Barticevic[2]

[1] *Facultad de Ingeniería, Universidad Diego Portales, Ejército 441 Santiago, Chile*
[2] *Departamento de Física, Universidad Técnica F. Santa María, Casilla 110 V, Valparaíso, Chile*

This paper presents a theoretical study of the implementation of an architecture of a quantum cellular automaton on a graphene nanoribbon. The cells of the automaton are made up by ^{13}C atoms and hydrogen atoms and the interaction between neighboring cells corresponds to the indirect coupling between nuclear spins. We have determined the relevant parameters characterizing the physical system for nuclear magnetic resonance and from knowledge of these parameters we have designed control protocols to study the evolution of the information through the quantum cellular automaton. Our results show that a graphene nanoribbon enriched with atoms of ^{13}C stores and processes quantum information in times less than the corresponding system decoherence times.

Keywords: Quantum Information, Cellular Automata, Graphene Nanoribbons.

RESEARCH ARTICLE

1. INTRODUCTION

A classical cellular automata is a structure of cells whose global evolution obeys local rules. This mathematical model proposed by Von Neumann[1] has been used to study physical and biological systems highly complex.[2] Each cell has a set of possible states, whose evolution depends on the state of the cell and the state of their neighboring cells. The shape of the update function depends on the system we wish to model. In 1982 Feynman studied the possibility of using cellular automata as models of quantum systems and as architecture of quantum computing.[3] From that date it has been discussed various models of quantum cellular automata (QCA) and its implementation for solving particular problems of computation.[4–23] An interesting type of model is to build a one-dimensional QCA architecture, with more than one qubit per cell,[24,25] which would be unaffected by the "no-go lemma"[26] which establishes that, except for the trivial case, the unitary evolution in a one-dimensional QCA is not possible. In this work we discuss, from the theoretical point of view, the implementation on a physical system, of a model that belongs to this latter type with some important variations.

The physical system on which the QCA will be implemented is a flat structure consisting of a segment of graphene, enriched with ^{13}C atoms. The ribbon width is of the order of 10 Å and variable length between 15 Å to hundreds of Å, with longitudinal zig–zag edges passivated with hydrogen atoms. The qubits contained in the cells correspond to the nuclear spins of the hydrogen atoms and ^{13}C atoms. The interaction between neighboring cells will be provided by the indirect coupling between the spins and we will use nuclear magnetic resonance (NMR) control operations to prepare the automata in a initial state and to generate the update function of each cell.

2. CHARACTERIZATION OF THE QCA ARCHITECTURE

Figure 1 shows a polycyclic aromatic hydrocarbon $C_{76}H_{26}$ enriched with ^{13}C atoms at the edge. This macromolecule can be visualized as a graphene nanoribbon (GNR) of finite length and passivated at the edges with hydrogen atoms. Nowadays, there are techniques to enrich carbon structures with the isotope ^{13}C in a controlled way,[27,28] this would allow to have atoms active for NMR in a desired place in the GNR. If this would not be possible, one can use control techniques of spins disconnection for holding an arbitrary structure in the nanoribbon.

Figure 2 shows a diagram of the model of QCA that we will developed on the carbon nanostructure. We can see in this pattern a set of two quantum entities (control qubit H and state qubit A) connected to a similar set through a cell with a single element (auxiliary qubit B). The cells of our QCA are formed by the qubits H and A, and Figure 3 shows the implementation of our model in one of the edges

*Author to whom correspondence should be addressed.

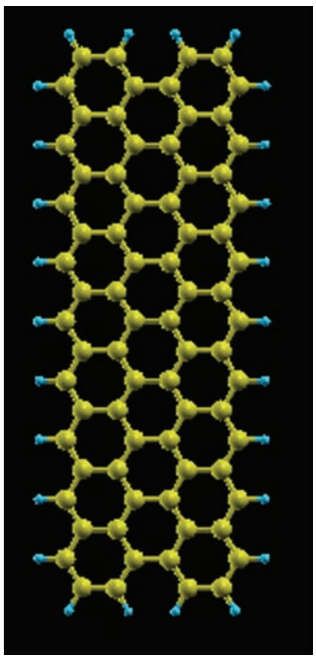

Fig. 1. Segment of a GNR passivated with hydrogen atoms at the edges.

of the molecule. To study the automaton evolution we must establish the corresponding nuclear spin Hamiltonian. For that we must determine the resonant frequency of each active nucleus and the coupling between those nuclei that are part of the automaton.

We consider a matrix of graphene nanoribbons with equal topological characteristics (subunits of the central processor) on an inert substrate, as shown in Figure 4. The whole system rotates to high frequency, around the magic angle (MAS) on the direction of the applied static magnetic field. This means that the dipolar coupling term between the spins can neglected. Thus the Hamiltonian of N spins can be written:

$$H = \sum_i \frac{\hbar\omega_i}{2} Z_i + \sum_{ij} \frac{2\pi}{\hbar} (\gamma_i \gamma_j)^{-1} \mu_i J_{ij} \mu_j + \sum_i C[X_i \cos(\omega_{rf} t) + Y_i \sin(\omega_{rf} t)] \quad (1)$$

where X_i, Y_i, Z_i are Pauli matrixes and the constant C depends on the magnitude of the control electromagnetic field amplitude which oscillates with frequency ω_{rf}.

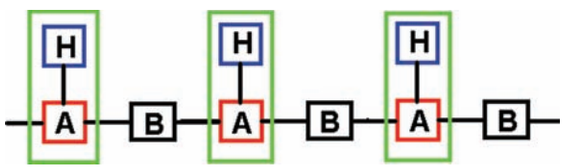

Fig. 2. Sketch of the QCA. The cells consist of the qubits H and A connected together through the qubit B.

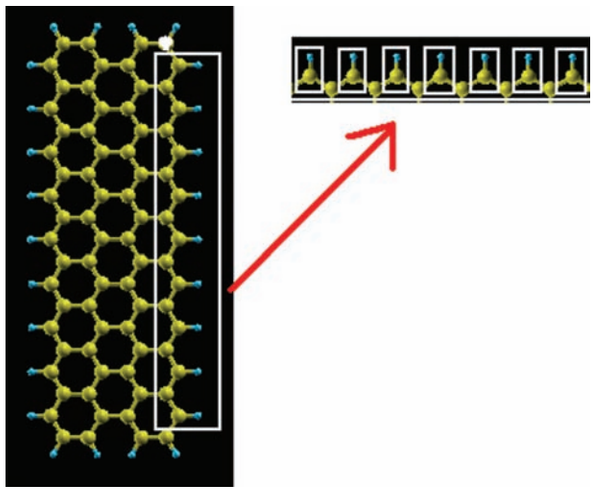

Fig. 3. Implementation of the QCA on the nanoribbons. The qubit H corresponds to the hydrogen atoms, the qubit A to the carbon atom bound to the hydrogen atom and, the qubit B to the carbon atom connecting the cells.

The second term of the Hamiltonian, $\mu_i = \gamma_i \hbar I_i$, corresponds to the nuclear magnetic dipole moment with γ_i being the gyromagnetic ratio and I_i, the nuclear spin angular momentum operator. The isotropic Larmor frequency ω_i can be determined by calculating the "nuclear shielding tensor" σ_i by means of the relation $\mu_i(1-\sigma_i)/2 = (\hbar\omega_i/2)Z_i$.

Finally, to determine the tensor coupling J_{ij} we must determine the "indirect reduced coupling tensor" K_{ij} which is related to the magnitude physically measured in the laboratory J_{ij}, through the equation $J_{ij} = (\hbar/2\pi)\gamma_i\gamma_j K_{ij}$. Then, calculating the tensors K_{ij} and σ_i we know all the terms of the Hamiltonian and thus we can design control protocols to program the evolution of the QCA. The QCA length determines the length of the GNRs, or its region of operation. With the idea to illustrate the dynamics of this architecture we will limit the QCA to the set of cells shown in Figure 3. All atoms from the edge of the ribbon correspond to isotopes ^{13}C and other atoms of the molecule that are outside the rectangle (and therefore outside the automaton) correspond to ^{12}C, inactive in NMR. The qubits involved in the QCA will be denominated HABHABHAB…, where H are hydrogen atoms, A the carbon atoms connected to them and B the central carbon atom.

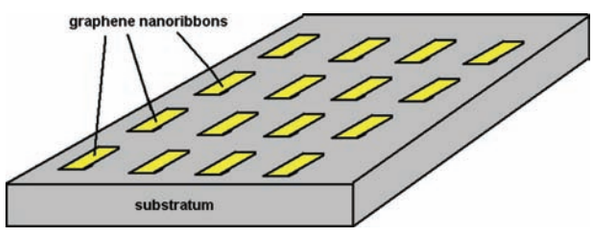

Fig. 4. Graphene ribbons matrix on an inert substrate.

To determine the tensors K_{ij} and σ_i, we first optimize the geometry of the system postulated by means of the method "quasi Newton approach"[29] then, we calculate the total energy of the system using first-principles calculations based on the density functional GGA Becke-Perdew.[30, 31] We use Slater type orbitals and double zeta polarized basis (DZP), by using the ADF software.[32] Finally, the shielding and indirect coupling tensors for the molecule are obtained as double first-order perturbations of the total energy $E = \langle\Psi|H|\Psi\rangle$ of the molecule.[33] The technical details of the calculation, additional terms in the Hamiltonian are discussed in a previous report[34] where we show calculations for the J coupling and chemical shifts of carbon-based nanostructures for NMR quantum computing.

Figure 5 shows the chemical shifts relative to the value for tetramethylsilane (TMS) computed at the same level of theory. In this figure we see that the hydrogens have resonance frequencies at the same position and that the external carbon atoms (A) coincide in the spectrum, its signal being slightly shifted from the internal carbon atoms (B). While the difference in frequency between external and internal carbons is small, it is enough to manipulate them separately with pulses of control for each spin. Of course, this behavior is valid over all the automaton (edge of the molecule), such that only there are three non-equivalent atoms in the automaton spectrum.

The results of the coupling tensor calculations gave the values of $J_1 = 158.3$ Hz between the atoms of hydrogen and external carbon atoms and $J_2 = 46.6$ Hz for the neighbors. The rest of the couplings are negligible with respect to these values, so we only consider interaction to nearest neighbors. Anyway the update function considers the fact that when the hydrogen atom interacts with the external carbon (A), the internal carbon atom (B) remains disconnected. In turn, when the carbon atoms interact, hydrogen will be disconnected. With the information about the couplings and the position of the spins in the spectrum, we can design a complete NMR control protocol that defines the update function of the automata. Thus the Hamiltonian of the system, without the control pulses, can be written:

$$H = -\frac{\hbar\omega_H}{2}\sum_i Z_i^H - \frac{\hbar\omega_A}{2}\sum_j Z_j^A - \frac{\hbar\omega_B}{2}\sum_k Z_k^B + \frac{\pi\hbar}{2}\left\{J_1\sum_{ij} Z_i^H Z_j^A + J_2\sum_{jk} Z_j^A Z_k^B\right\} \quad (2)$$

3. DYNAMICS SIMULATION OF THE QCA

We will make a proof of concept to illustrate the dynamic behavior of the QCA. To load and read data into the automaton, we use an additional atom ^{13}C in one of the corners of the molecule. The position in the molecule of this atom is illustrated in Figure 3, in the upper right corner (white in the diagram). The resonant frequency of this spin is slightly different from the carbon atom A and it is only connected to a carbon atom B.[34] The control over the atom will allow us to carry information in the automaton and, after this information is processed it can be read. The study of such kind of structures[34] indicates that the resonant frequency of the hydrogen bound to the atom of the end of the array is the same as the rest of the hydrogen atoms in the automaton.

The automaton update function will be based on a sequence of pulses with frequencies ω_H, ω_A and ω_B displaced by an amount that is a function of the value of the spin of neighboring atoms. For example, let us assign the vector $|0\rangle$ to the lowest energy level and $|1\rangle$ to the excited state. When the hydrogen atoms are disconnected, the configurations of the first neighbors to the atom A will be the following $0A0, 0A1, 1A0, 1A1$. Similarly one has the configuration for atoms B. From the first principles calculations we simulated the spectrum of atoms A and B in a 300 MHz spectrometer. The simulation is shown in

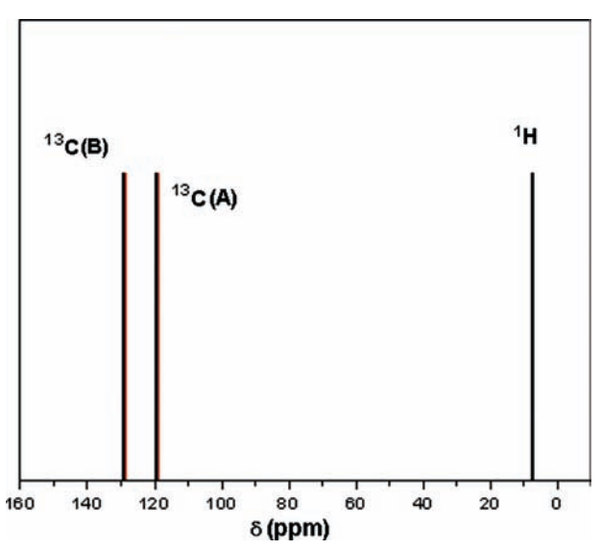

Fig. 5. Chemical shifts relative to the TMS value.

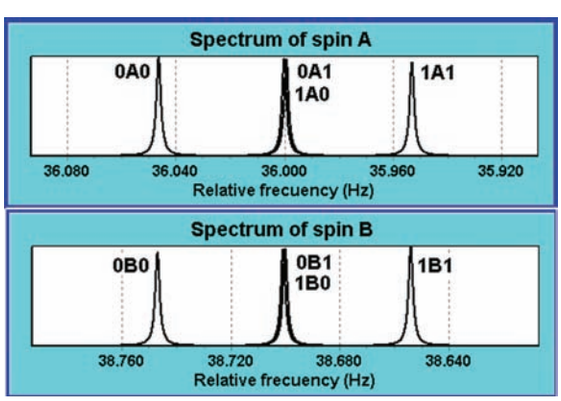

Fig. 6. Spectrum of atoms A and B in a 300 MHz spectrometer.

RESEARCH ARTICLE

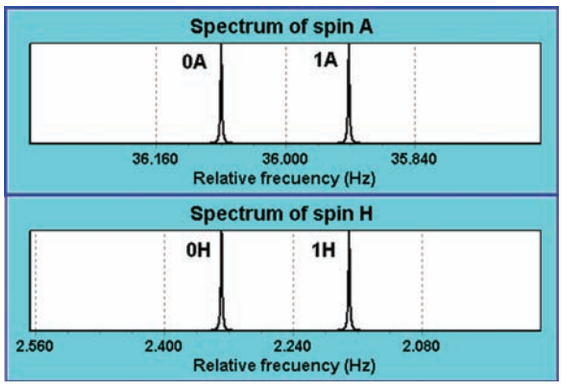

Fig. 7. Spectrum of atoms A and H in a 300 MHz spectrometer.

Figure 6. We can say that the field generated by the neighboring spins has three values, 0, 1 and 2 (resulting from adding the 0 and 1 neighbors). This implies that we can manipulate atoms A and B with pulses to rotate the spin with frequencies $\omega_A^0, \omega_A^1, \omega_A^2, \omega_B^0, \omega_B^1$ and ω_B^2 where the super index indicates the field generated by the neighbors. This is completely analogous to the case of the spin B disconnected and the control qubit H interacts with the qubit state A. Our results also allow to simulate the spectrum of these atoms in the spectrometer 300 MHZ. Figure 7 shows these results.

3.1. Procedure for Charging and Reading Data

Lets suppose the initial state of the system corresponds to put all spins in the lowest energy level $|0\rangle$ (this initial assumption will be discussed in the section of analysis of errors). Figure 8 shows the protocol used to carry information in the automaton from the initial state $|000.0\rangle$. This procedure was discussed in the Lloyd's abstract model,[16] which differs from this in the disposition of the quantum entities. The atom labeled with the letter C (left in the diagram) corresponds to the spin at the end of the automata. On the right side of the diagram of Figure 8 can be appreciated the pulse sequence that allows us to

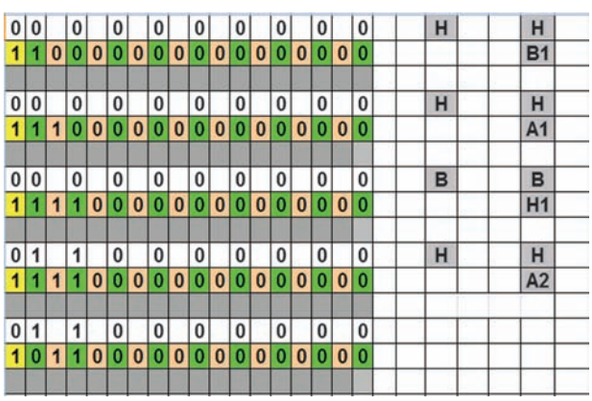

Fig. 8. Procedure to load data.

charge information in the automaton. The pulses of the first row (in each sequence) are triggered in the middle and the end of time interval considered for the update. These pulses indicate a rotation π of the atom considered and obey the usual protocol for disconnection of spins (refocusing). The bottom row in each step indicates the pulse to move the bit information to the right of the automata. The notation $A1$ indicates a pulse π on the atom A if the field on this atom is 1. Figure 8 shows that in the first 4 update steps of the automaton the hydrogen is hold disconnected and the first three carbon qubits are changed from 0 to 1. After the sixth step of updating the vector describing the state of the automaton $|\text{HCHABHAB}\ldots\rangle$ has changed from the state $|0000000\ldots0\rangle$ to the state $|011011100\ldots0\rangle$. Depending on the configuration we like to have loaded in the automaton, it should develop the protocol pulses that lead to that configuration. If you have N_0 copies of the molecule in the system (CPU subunits), the pulses live N_0 automata with the same configuration of information.

Besides to the classical information loaded in the automaton, we may charge actual quantum states by using an appropriate protocol of pulses. For example if we apply a pulse at the beginning of $\pi/2$ with frequency ω_C^0 and length t_0, the qubit we will leave the end qubit (atom C) in the state $1/\sqrt{2}(|0\rangle + e^{-i\phi_1}|1\rangle)$, where $\phi_1 = \pi/2 + \omega_C^0 t_0$. Then by using more pulses we can put the neighboring qubits in a superposition of states.

To read the data it must interact with only one copy of automata (subunit). We move the qubit to be read to the end of the automata and then to apply two pulses π with frequencies $\omega_C^{0,1}$ and then wait to see if a pulse is attenuated or amplified.[16] Depending on this we will know if the bit moved to the end is in a state $|0\rangle$ or $|1\rangle$. The number of copies of the automata allows to read the various qubits of information.

3.2. Quantum Computation

Quantum computing operations can be performed by using unit operations between cells of the automaton. It was shown in the former section that with a suitable pulse protocol we can move one state vector to another of the system and this would correspond to a unitary transformation. To generalize this type of operation we can proceed as in the abstract models of Benjamin,[14–15] where a subset of the QCA cells are used as qubits of information separated by qubits in only one possible state. In these models one or more control units are used to process the information. In our model the control units correspond to the atoms of hydrogen attached to atoms A of the automaton. A specific procedure with the model used in this work is to store data with ramdom pulses (of $\pi/2$ for example) to create EPR states between the qubits state and in this way the information can be read only by the person responsible

to charge this information and knows the pulse sequence. That is, we can use this system to store encoded data with maximum safety.

4. MODEL SCALABILITY

The implementation of the QCA model on the edge of the nanoribbons presents the advantage of scalability in the number of qubits. By considering atom of the end of automaton (atom C), we have only 4 nonequivalent spins in the system, independent of the number of qubits that form the automaton and therefore independent of the molecule length. We can work with hundreds or thousands of spins, but we should only handle 4 through global pulses and not individual ones.

On the other hand, it is required to work with redundant information to perform the data reading, that is, to have a certain amount of copies the same automaton. If we increase the number of qubits in the automaton, we should proportionally increase the number of copies of the nanoribbons.

5. SOURCES OF ERROR

One of the most important sources of errors in the implementation of our model in graphene nanoribbons supported in a substrate is the manipulation through pulses of the individual subsystems to read the processed information. This involves to localize the beam pulse in a region of a few $(\text{nm})^2$ on the matrix that is spinning in the laboratory reference system. The errors coming from this situation can be reduced taking the source of pulsing radiation in the framework of the substrate, i.e., rotating with the processor.

Another possible source of error is the loss of efficiency of the pulses when they are directed to only one type of atom. It is possible that another type of spins respond to these pulses. This can be reduced with a precise knowledge of the resonance frequencies and coupling constants. In this work we simulated the spectrum of spins in a 300 MHz spectrometer which makes that the resonance frequencies are sufficiently separated in order to address the pulses efficiently.

The implementation of the model in the nanobelts have the problem of we are not working with an ensemble of millions of molecules as in the case of NMR in dilute systems. This implies that the signal output is extremely weak and therefore should be available an adequate system for high fidelity amplification, such as personal used in optical cavities. Finally it is important to note that the implementation is perform at low temperature to have the automata in a state initial rate $|000000\ldots0\rangle$.

All these sources of error can be managed and controlled for working with this system under the cellular automaton architecture. The justification for implementing this model in the graphene nanoribbons, considering the sources of errors is detailed in following points:

(1) Today there are synthesis techniques that allows to have a regular arrangement of graphene nanoribbons doped with ^{13}C.[27, 28, 34]

(2) The regular array system $C_N H_M$ allows for a number of processors that store the same information. This redundant storage allows the data reading and the processing of errors.

(3) The scalability of automata with the number of qubits allows the processing of large amount of information. This is of vital importance for programing the protocols of errors correction. In this model the standard errors correction codes[36] were used, which implies to have redundant data within the automaton, for example the qubit sequence shown in Figure 9 would be representing the repetition of information, an encoded cell corresponding to the union of two original cells of the automaton. This allows a robust error correction procedure. The fault-tolerant operations are programmed as a set of pulses to develop unit operations, manipulating this redundant information.

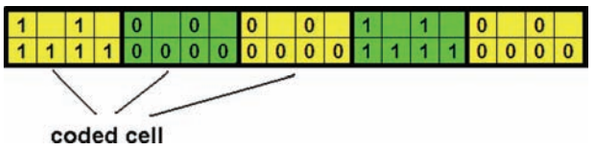

Fig. 9. Repeat sequence of qubits for error correction.

6. CONCLUSIONS

This paper presents a theoretical study of quantum cellular automata model and its implementation in a physical system formed by an array of graphene nanoribbons. The qubits of the automaton correspond to the nuclear spins of the atoms of ^{13}C and atoms of ^{1}H present at the edges of the ribbon. Using first principle calculations and perturbation theory the frequencies of resonance and the coupling constants were determined. From these calculations we can design the pulse protocols to load and read information in the automaton and to process this information. The sources of error present in the implementation of the model in the physical system are easy to operate with the usual protocols of error correction. We conclude that this system is a good candidate for quantum information processing at low temperature. Calculations on the dynamic behavior of the automaton as a function of temperature are currently performed and will be published in the next future.

Acknowledgments: The authors acknowledge the financial support of FONDECYT program grants 1100672, 11100045 and USM 110971 internal grant.

References

1. J. von Neumann, Theory of Self-Reproducing Automata, University of Illinois Press, Urbana, IL (**1966**).

RESEARCH ARTICLE

2. D. Griffeath and C. Moore, New Constrictions in Cellular Automata, University Press, Oxford, **(2003)**.
3. R. P. Feynman, *Int. J. Phys.* 21, 467 **(1982)**.
4. B. Schumacher and R. F. Werner **(2004)**, quant-ph/0405174.
5. W. van Dam, Master's Thesis, University of Nijmegen **(1996)**.
6. J. Watrous, *Proceedings of the 36th Annual Symposium on Foundations of Computer Science (FOCS)* **(1995)**, pp. 528–537.
7. C. A. Perez-Delgado and D. Cheung **(2005)**, quant-ph/0508164.
8. G. Grossing and A. Zeilinger, *Complex Systems* 2, 197 **(1988)**.
9. D. A. Meyer, *Journal of Statistical Physics* 85, 551 **(1996)**.
10. B. M. Boghosian and W. Taylor, *Phys. Rev. E* 57, 54 **(1998)**.
11. D. M. Forrester, K. E. Kurten, and F. V. Kusmartsev, *Phys. Rev. B* 75, 014416 **(2007)**.
12. J. Fitzsimons and J. Twamley, *Phys. Rev. Lett.* 97, 090502 **(2006)**.
13. K. G. H. Vollbrecht and J. I. Cirac, *Phys. Rev. A* 73, 012324 **(2006)**.
14. S. C. Benjamin, *Phys. Rev. A* 61, 020301 (R) **(2000)**, quant-ph/9909007.
15. S. C. Benjamin and S. Bose, *Phys. Rev. Lett.* 90, 247901 **(2003)**.
16. S. Lloyd, *Science* 261, 1569 **(1993)**.
17. R. Raussendorf, *Phys. Rev. A* 72, 022301 **(2005)**.
18. D. J. Shepherd, T. Franz, and R. F. Werner, *Phys. Rev. Lett.* 97, 020502 **(2006)**.
19. A. Imre, G. Csaba, L. Ji, A. Orlov, G. H. Bernstein, and W. Porod, *Science* 311, 205 **(2006)**.
20. M. Khatun, T. Barclay, I. Sturzu, and P. D. Tougaw, *J. Appl. Phys.* 98, 094904 **(2005)**.
21. C. A. Perez-Delgado, M. Mosca, P. Cappellaro, and D. G. Cory, *Phys. Rev. Lett.* 97, 100501 **(2006)**.
22. K. Walus and G. A. Jullien, *Proceedings of the IEEE* 94, 1225 **(2006)**.
23. P. J. Love and B. Boghosian, *Physica A* 362, 210 **(2006)**.
24. I. G. Karafyllidis, *Phys. Lett. A* 320, 35 **(2003)**.
25. I. G. Karafyllidis, *Phys. Rev. A* 70, 044301 **(2004)**.
26. S. Fussy, G. Grössing, H. Schwabl, and A. Scrinzi, *Phys. Rev. A* 48, 3470 **(1993)**.
27. W. Cai, et al., *Science* 321, 5897 **(2008)**.
28. A. J. Heinrich, C. P. Lutz, J. A. Gupta, and D. M. Eigler, *Science* 298, 1381 **(2002)**.
29. L. Versluis, The Determination of Molecular Structures by the HFS Method, University of Calgary **(1989)**.
30. A. D. Becke, *Phys. Rev. A* 38, 3098 **(1988)**.
31. J. P. Perdew, *Phys. Rev. B* 33, 8822 **(1986)**.
32. http://www.scm.com/.
33. J. Autschbach, *Structure and Bonding* 112 **(2004)**.
34. A. León, Z. Barticevic, and M. Pacheco, *Chem. Phys. Lett.* 470, 249 **(2009)**.
35. L. M. K. Vandersypen and I. L. Chuang, *Rev. Mod. Phys.* 76, 1037 **(2005)**.
36. M. A. Nielsen and I. L. Chaung, Quantum Computation and Quantum Information, Cambridge University Press, Cambrige **(2003)**.

Received: 4 June 2011. Accepted: 3 July 2011.

RESEARCH ARTICLE